

Nonlinear Deformation Processes and Damage Modes of Super Carbon Nanotubes with Armchair-Armchair Topology *

CHEN Yu-Li(陈玉丽)¹, LIU Bin(刘彬)^{1,2}, YIN Ya-Jun(殷雅俊)^{1**}, HUANG Yong-Gang(黄永刚)³,
HWUANG Keh-Chih(黄克智)¹

¹FML, Department of Engineering Mechanics, Tsinghua University, Beijing 100084

²State Key Laboratory of Structural Analysis for Industrial Equipment, Dalian University of Technology, Dalian 116023

³Department of Civil and Environmental Engineering and Department of Mechanical Engineering, Northwestern University, Evanston, Illinois 60208, USA

(Received 27 March 2008)

The tensile deformations and fractures of super carbon nanotubes (SCNTs) with armchair-armchair topology are investigated by using the atomic-scale finite element method. SCNTs generated from carbon nanotubes (CNTs) with different characteristic aspect ratios are found to have different nonlinear behaviours under uniaxial tensions. Specifically, an SCNT with higher aspect ratio has three distinct stages: rotation, stretch and rupture, while an SCNT with lower aspect ratio has only two stages. This information may compensate for previous work and enrich our knowledge about Y-branched CNTs and SCNTs.

PACS: 61.46.Fg, 81.07.De, 61.46. –w

In 1995, Zhou *et al.*^[1] observed branched CNTs with L, Y and T patterns in experiments. These carbon nanostructures have been used as multi-terminal electronic devices and circuits.^[2,3] Among them, Y-branched CNTs have drawn intense attentions,^[4–13] because their symmetrical structures are possible to act as new nanotube-based network.^[14,15]

On the basis of symmetric Y-branched CNTs, a novel carbon nanostructure called super carbon nanotube (SCNT) is published recently.^[16,17] A super carbon nanotube may be generated through replacing the carbon-carbon bonds and carbon atoms of a carbon nanotube respectively by smaller carbon nanotubes and Y-branched junctions.^[16] Yin *et al.*^[17] theoretically prove that spontaneous Y-branched CNTs may have both minimum energy and symmetric geometry.

Such beautiful carbon nanostructures have drawn the attentions of researchers. Pugno^[18] studied the mimicking nacre with SCNTs for producing optimized super-composites. Wang *et al.*^[19] simulated the mechanical properties of the super graphite (SG), from which SCNTs may be made. Qin *et al.*^[20] predicted the superior flexibility of the SCNTs through molecular dynamics simulations. However, there have been few researchers exploring the influences of the aspect ratios of CNT on the global deformation and damage modes of SCNTs. In this Letter, we try to compensate for this weak point by the atomic-scale finite element method (AFEM).^[21,22]

Generally speaking, molecule dynamics (MD) method is also widely used to simulate the mechanical properties of CNT. According to Refs. [21,22], the AFEM is of the same accuracy as MD, but takes less CPU than MD. For quasi-static processes of atomic

systems, the AFEM is an effective and robust atomistic simulation method. Therefore, the AFEM instead of MD is used in numerical simulations in this study.

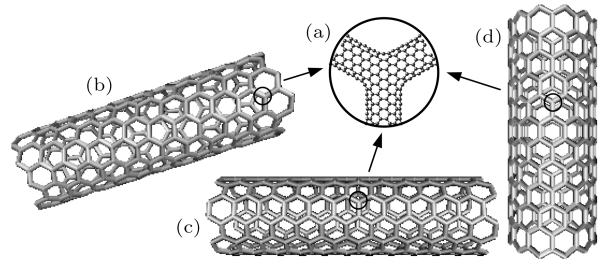


Fig. 1. Super carbon nanotubes with Scuseria-type Y-branched junctions: (a) Scuseria-type Y-branched junction, (b) armchair-chirality topology, (c) armchair-armchair topology, and (d) armchair-zigzag topology.

There are three types of CNTs, i.e. zigzag, armchair and chirality. Theoretically there are also three types of SCNTs, each of which might be formed by three types of common CNT “arms” and the corresponding Y-branched junctions. Hence, there are totally nine types of topologies for SCNTs. Scuseria^[4] proposed a kind of symmetric Y-branched junction with armchair topology, composed of heptagons at the connected junction [Fig. 1(a)]. If the armchair CNTs are connected with the Scuseria-type Y-branched junctions, the SCNTs with armchair-chirality [Fig. 1(b)], armchair-armchair [Fig. 1(c)] and armchair-zigzag [Fig. 1(d)] topologies may be formed. In this work, SCNTs with armchair-armchair topology are studied.

*Supported by the National Natural Science Foundation of China under Grant Nos 10542001 and 10572076.

**Email: yinyj@mail.tsinghua.edu.cn

© 2008 Chinese Physical Society and IOP Publishing Ltd

The Y-branched CNT [Figs. 2(b) and 2(c)] may be considered as the representative cell element for the super graphite (SG). As reported by Wang *et al.*,^[23] the mechanical properties of the CNT are similar to that of the graphite sheet when the number of carbon atoms along the circumference is large enough. Analogously, the mechanical properties of SCNTs may be very near to that of the SG when the number of Y-junctions along the circumference is large enough. If the behaviours of Y-branched CNTs [Fig. 2(c)] are clearly understood, the mechanical properties of the SCNTs may be evaluated. Therefore, we concentrate on the Y-branched CNT or the representative cell element in Fig. 2(b).

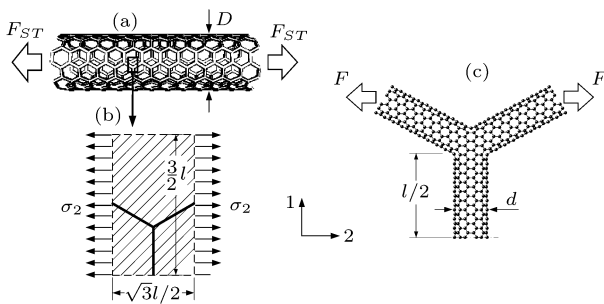


Fig. 2. Simulation model for a super carbon nanotube with armchair-armchair topology: (a) super carbon nanotube under uniaxial tension, (b) the representative cell element of the super carbon nanotube, and (c) the atomic model for AFEM simulations.

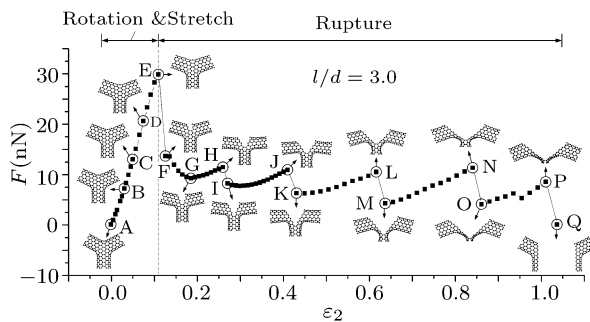


Fig. 3. Typical nonlinear deformation and damage processes of Y-branched CNT with low aspect ratio $l/d = 3$.

The arm length of CNTs in the SCNT shown in Fig. 2 is l , and the arm length of the Y-branched CNT in the cell element is then $l/2$. The length and width of the cell element are $\sqrt{3}l/2$ and $3l/2$ respectively [Fig. 2(b)]. The atomic model is presented in Fig. 2(c). The Y-branched CNTs are constituted by Scuseria-type junctions [Fig. 1(a)] and (6, 6) CNTs. Three typical aspect ratios (l/d) are taken to be 3, 6 and 24 respectively. The uniaxial tension force F is applied along direction 2. This means that the ends of the upper two arms of the Y-branched CNT are tensioned by a pair of forces with the same value of F but in the opposite directions. The displacements along direction

1 are free from constraint. In the AFEM^[21,22] the modified second-generation Brenner potential^[24] and Lennard-Jones 6–12 potential are used to describe the energies of C–C covalent bonds and van der Waals interactions, respectively.

Figures 3 and 4 show the two types of typical nonlinear deformation and damage processes of the cell element. They are analysed in the following.

When the aspect ratio is low ($l/d = 3$), two stages are disclosed in the deformation and damage processes (Fig. 3). The first stage ranges from point A to point E, which is a perfect linear stage with large slope. In this stage, the two upper arms look like two short "beams" connected to the junction. The junction can be viewed as a spiral spring since the angle constraint due to the covalent bonds and van der Waals interactions among atoms are not rigid. In other words, the two beams bear both bending and stretching deformations. In the loading process, both rotation and stretch develop simultaneously. Moreover, the rigidity of the cell element with low aspect ratio is large, so the bending deformation (or rotation) is difficult. Along with the increase of the strain in direction 2, the rotation of the two upper arms becomes more and more difficult. If the two upper arms move parallel with each other, their rotations may be baffled by the covalent bonds among atoms. At point E, the first stage is finished and the force reaches the maximum value $F_E = F_{\max} \approx 29.8$ nN and the strain approaches $\varepsilon_E \approx 11.1\%$.

From point E, the second deformation stage is initiated. This stage looks very complicated but obeys some rules. It includes a few deformation periods. In every period there are two deformation steps. Some of the steps are accompanied by the changes of topologies or ruptures in the Y-branched junction. The first period is E→G→H. The point E is a critical point at where the initial rupture occurs: The bonds begin to break from the centre of the Y-branched junction. After that, the force suddenly drops to point F with $\varepsilon_F \approx 12.7\%$ and $F_F \approx 13.6$ nN. This sudden drop comes from the continuous breakages of bonds and the propagations cracks. However, the state at point F is not stable, and the crack continues to propagate vertically to the tension direction. Fortunately, this unstable propagation can not be progressed forever. There is a mechanism of brake to the propagations of the cracks: At point G, the crack is stopped when it goes through the junction and approaches to the lower arm, and the force drops to the local lowest value $F_G \approx 9.6$ nN. Then, another step, i.e. G→H, occurs. The G→H step is a reloading and hardening one inside which stretching deformations in both the upper arms and the tips of the crack are developed. In this step, no breakage of bonds and change in topology occur. The E→G→H forms a complete fracture and deformation period. Point H is also a critical point

from where another complete fracture and deformation period $H \rightarrow I \rightarrow J$ is started. Different from the former period ($E \rightarrow G \rightarrow H$), only one pair of bonds breaks in this period, and so do the following three periods ($J \rightarrow K \rightarrow L$, $L \rightarrow M \rightarrow N$, and $N \rightarrow O \rightarrow P$). From point P, the last period begins. However, this period is not finished, because the last pair of remained bonds is penetrated by the tips of the crack, and the Y-branched CNT is separated into two parts at point Q, which finally ends the third stage. It is noted that the surfaces of the two symmetric cracks are very smooth, and their propagation direction keeps in the vertical one. We may roughly say that the crack is of “mode I” characteristics.

Lastly, the profile of the deformation curve in the third stage is of the wave-like or “zigzag” style. In appearance this stage is composed of a series of transitions “sudden unloading \rightarrow reloading \rightarrow sudden unloading \rightarrow reloading”. Practically this stage includes a series of transitions from “sudden softening \rightarrow hardening” and “dynamic cracking \rightarrow static stretching”.

When the aspect ratio is not too low ($l/d = 6$) or very high ($l/d = 24$), three stages are revealed in the deformation and damage processes [Figs. 4(a) and 4(b)]. The case of $l/d = 6$ in Fig. 4(a) is studied firstly.

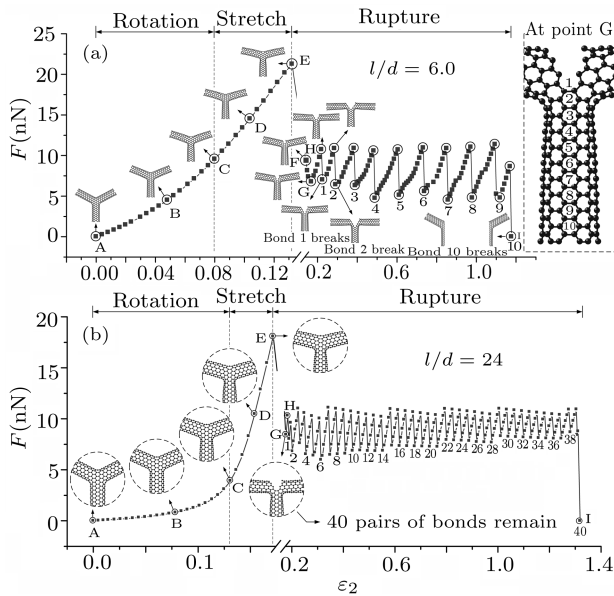


Fig. 4. Typical nonlinear deformation and damage processes of Y-branched CNT with high aspect ratio: (a) $l/d = 6$ and (b) $l/d = 24$.

The first stage ranges from point A to point C, which is a nonlinear curve with low but increasing slope. The second stage ranging from point C to point E is a perfect linear line with larger slope. The slope in the first stage is lower than the second one, because the beam with larger aspect ratio is easier to rotate and the Y-branched junction behaves relatively “softer”. Thus the tension force increases slowly along

with the increment of the strain. In this stage, the two upper arms jointed by the junction, or two beams connected by a spiral spring, mainly bear bending deformations. If we carefully check the profile of the two beams, we may find little stretching deformations but large bending deformations and intensive rotations relative to the horizontal axis. If the two upper arms move close enough to the horizontal direction (direction 2), their rotations may be baffled by the covalent bonds and van der Waals interactions among atoms, and further rotations become more and more difficult. When the difficulty of bending is comparative to the difficulty of stretch, the first stage is transited into the second one gradually.

Along with the increasing of the force, the shrinkage of the lower arm in the connecting region becomes more and more obvious. If we check the section of this region [Fig. 5(a)] carefully, the deformation mechanism is revealed. The transition process of the section in this case is shown in Fig. 5(c). Before loading, there is no force on the Y-branched CNT (at point A), and the section is round. After loading, because of the rotation of the two upper arms, the lower arm is squeezed and compressed, and the section becomes an ellipse (take point B as example). If the compression on the ellipse section is large enough, the convex surface changes to be concave, and the ellipse changes into the dumbbell shape (take point D as example). The concave surface leads to the increase in the junction bending stiffness. Hence, the critical point from convex to concave (i.e. point C with $F_C \approx 9.6$ nN and $\varepsilon_C \approx 8.0\%$) should be the boundary between the two stages.

From point C to point E, we obtain the second stage of the deformation curve. In this stage, the bending-dominant-deformation mode in the first stage is converted into the stretching-dominant-deformation mode in the second stage, because the rotation deformation is much more difficult in the second stage. Therefore, the hardening effect and large slope may come from both the stretch of the arms and the resistance of the Y-branched junction to the angle change. When the deformation reaches point E, the two upper arms are almost parallel to the tension direction, and the tension force approaches the maximum value ($F_{\max} \approx 21.3$ nN). The second stage stops at the point E with $\varepsilon_E \approx 13.2\%$ and $F_E = F_{\max} \approx 21.3$ nN.

It is interesting to note that the obvious differences of the slopes between the first and the second stages are not found in the previous case of low aspect ratio. If we check the section of lower arm in the connecting region in the case of low aspect ratio, we may also find a critical point [Fig. 5(b), point C]. Before this point, we should see the bending-dominant-deformation mode, but the rotation is so difficult that both the bending deformation and stretch deformation are comparable and develop simultaneously.

The third stage in the case of high aspect ratio is similar to those of the low aspect ratio. It starts from point E, and also includes a few characteristic periods. Point E is the critical point for initial fracture. After a series of bond breakages, the force drops to the local lowest value ($F_G \approx 6.8$ nN) at point G, and the crack is stopped when it approaches the lower arm. Then, a reloading and hardening step (G→H)

without any changes in topology occurs. From H to I, a series of sudden unloading → reloading periods are presented. Each period corresponds to the breakage of one pair of bonds, and the bond pairs 1 to 10 break in sequence. It is noted that the number of periods is equal to the number of bond pairs along the path of crack propagation.

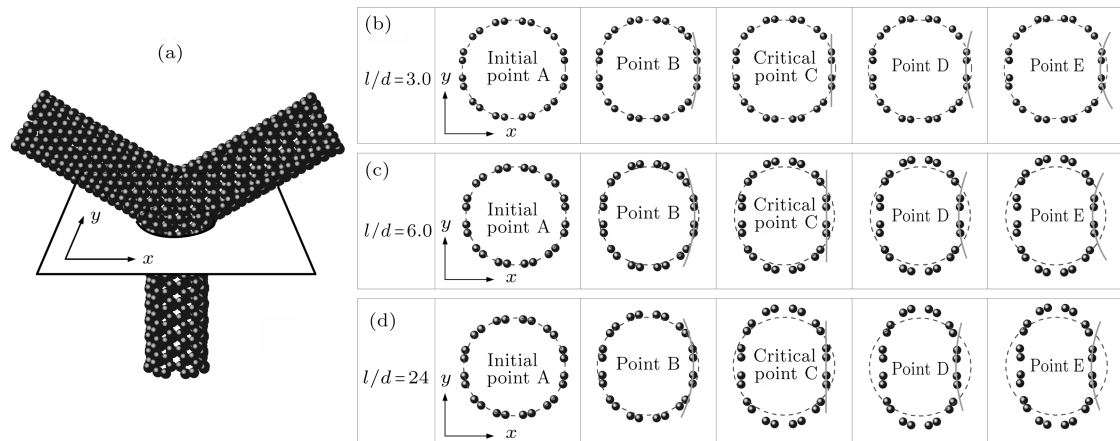


Fig. 5. Shrinking section of the lower arm in the connecting region: (a) position of the section, (b) $l/d = 3$, (c) $l/d = 6$ and (d) $l/d = 24$.

Figure 4(b) shows that the case of $l/d = 24$ is similar to the case of $l/d = 6$. This reveals the following meanings: If the aspect ratio is not too low (not lower than 6), the deformation and damage processes may obey the similar rules. Further more, in the third stage, the number of sudden unloading → reloading periods is linear proportional to the aspect ratio [see Figs. 4(a) and 4(b)].

From Figs. 3 and 4(a) to 4(b), we can find that the damage mode varies gradually along with the aspect ratio. In other words, there is no obvious critical aspect ratio at where the damage mode is suddenly shifted from one type to another.

In summary, the two representative nonlinear processes simulated by the atomic-scale finite element method in Figs. 3 and 4 reveal plentiful information about the deformation and damage of Y-branched CNT and the ST with armchair-armchair topology under uniaxial tension. Several differences and similarities between the SCNTs with smaller aspect ratio in Fig. 3 and larger ones in Fig. 4 are found: (1) The latter have three stages: rotation, stretch and rupture, while the former has only two stages because the rotation and stretch stages are merged. (2) In the first stage, the former has higher slope, which indicates that the slope decreases along with the increase of the aspect ratio. (3) In the last stage, the latter have longer process, but both of them obey the same rules: (a) The tension-extension curves after the bond breaking are of the zigzag feature. (b) The cracks propagate as the fracture mode I. (c) After the crack tip approaches the lower arm, the number of zigzags in the

curves (or sudden unloading → reloading periods) is linearly proportional to the aspect ratio.

The present results indicate that the CNT aspect ratio can affect the deformation and damage behaviours. The information presented here enriches our knowledge about Y-branched CNTs and SCNTs, and may lay the foundations for further explorations to their properties.

References

- [1] Zhou D and Seraphin S 1995 *Chem. Phys. Lett.* **238** 286
- [2] Chico L et al 1996 *Phys. Rev. Lett.* **76** 971
- [3] Terrones M et al 2002 *Phys. Rev. Lett.* **89** 075505
- [4] Scuseria G E 1992 *Chem. Phys. Lett.* **195** 534
- [5] Biro L P et al 2002 *Diam. Relat. Mater.* **11** 1081
- [6] Li J, Papadopoulos C and Xu J 1999 *Nature* **402** 253
- [7] Nagy P et al 2000 *Appl. Phys. A: Mater. Sci. Process.* **70** 481
- [8] Satishkumar B C et al 2000 *Appl. Phys. Lett.* **77** 2530
- [9] Gan B et al 2000 *Diam. Relat. Mater.* **9** 897
- [10] Gan B et al 2000 *Mater. Lett.* **45** 315
- [11] Deepak F L et al 2001 *Chem. Phys. Lett.* **345** 5
- [12] Li W Z et al 2001 *Appl. Phys. Lett.* **79** 1879
- [13] Ting J M and Chang C C 2002 *Appl. Phys. Lett.* **80** 324
- [14] Terrones M 2003 *Ann. Rev. Mater. Res.* **33** 419
- [15] Dag S et al 2004 *Phys. Rev. B* **70** 20540720
- [16] Coluci V R, Galv and Jorio A 2006 *Nanotechnology* **17** 617
- [17] Yin Y et al 2006 *Nanotechnology* **17** 4941
- [18] Pugno N M 2006 *Nanotechnology* **17** 5480
- [19] Wang M et al 2007 *Nanotechnology* **18** 075711
- [20] Qin Z et al 2007 *Appl. Phys. Lett.* **91** 043108
- [21] Liu B et al 2004 *Comput. Meth. Appl. Mech. Engin.* **193** 1849
- [22] Liu B et al 2005 *Phys. Rev. B* **72** 0354353
- [23] Wang L F et al 2005 *Phys. Rev. Lett.* **95** 10550110
- [24] Brenner D W et al 2002 *J. Phys.: Condens. Matter* **14** 783